Computers and Mathematics with Applications 61 (2011) 1217–1227

Contents lists available at ScienceDirect

Computers and Mathematics with Applications

journal homepage: www.elsevier.com/locate/camwa

Computational aspects of harmonic wavelet Galerkin methods and an application to a precipitation front propagation model

Saulo R.M. Barros *, Pedro S. Peixoto

Instituto de Matemática e Estatística - Universidade de São Paulo, R. do Matão 1010, 05508-090 São Paulo, Brazil

ARTICLE INFO

Article history:
Received 26 March 2010
Accepted 29 December 2010

Keywords:
Harmonic wavelets
Connection coefficients
Pseudo-spectral
Burgers equation
Computational complexity
Front propagation
Precipitation fronts
Wavelet Galerkin method

ABSTRACT

This article is dedicated to harmonic wavelet Galerkin methods for the solution of partial differential equations. Several variants of the method are proposed and analyzed, using the Burgers equation as a test model. The computational complexity can be reduced when the localization properties of the wavelets and restricted interactions between different scales are exploited. The resulting variants of the method have computational complexities ranging from $O(N^3)$ to $O(N)$ (N being the space dimension) per time step. A pseudo-spectral wavelet scheme is also described and compared to the methods based on connection coefficients. The harmonic wavelet Galerkin scheme is applied to a nonlinear model for the propagation of precipitation fronts, with the front locations being exposed in the sizes of the localized wavelet coefficients.

1. Introduction

The use of wavelets in Galerkin methods for the solution of partial differential equations often leads to computationally expensive schemes, although there are interesting possibilities to exploit the localization properties of the basis elements (see, e.g., [1–3]), also in combination with local refinement techniques [4,5]. High computational costs are mainly related to the connection coefficients in nonlinear equations, besides the solution costs. Complex harmonic wavelets [6] have a simple analytic expression, form an orthonormal basis and their frequency spectrum is band limited, although they do not have a compact support. The use of harmonic wavelets in Galerkin methods was first considered in [7] for the Burgers equation. More recently, they have been applied in the solution of other partial differential equations [8,9]. The analytic form of the harmonic wavelets allows the explicit derivation of their connection coefficients, used in the methods mentioned above.

The purpose of this article is to analyze the computational costs involved in harmonic wavelet Galerkin methods. For the nonlinear one-dimensional (1D) Burgers equation with diffusion, we consider different implementations, investigating the computational improvements possibly achieved by exploiting the localization properties of the wavelets along the same lines as proposed in [7], with some generalizations. In all variants analyzed, we deduce the computational complexity of the resulting method (varying from $O(N^3)$ to $O(N)$ per time step, N being the number of basis elements) and access the impacts in accuracy caused by the simplifications. As an alternative, we also consider pseudo-spectral implementations, pointing out advantages and disadvantages.

We employ the harmonic wavelets in a model for simulating precipitation fronts proposed in [10]. We show that the harmonic wavelets are able to capture the front locations very well, with a clear relation between spectral coefficients and the position of the fronts.

The remainder of this article is structured as follows. In Section 2, we describe the wavelet Galerkin method for the Burgers equation and its simplified variants, and we derive the computational complexity of the corresponding schemes. In

* Corresponding author. Tel.: +55 11 30916136; fax: +55 11 30916131.
E-mail addresses: saulo@ime.usp.br (S.R.M. Barros), pedrosp@ime.usp.br (P.S. Peixoto).

0898-1221/$ – see front matter © 2011 Elsevier Ltd. All rights reserved.
doi:10.1016/j.camwa.2010.12.073

Section 2, we also present the pseudo-spectral implementation and its costs, while several comparative results are shown in Section 3. Section 4 is dedicated to the wavelet scheme for simulating precipitation fronts and numerical results relating spectral coefficients and front locations. The paper is closed with some concluding remarks in Section 5.

2. Harmonic wavelets and Galerkin methods for the Burgers equation

Harmonic wavelets are complex orthonormal wavelets whose Fourier transforms are band limited [6]. They are closely related to Shannon, or *sinc*, wavelets. For our numerical purposes, we define (as in [11]) a periodized harmonic wavelet on [0, 1] as

$$\psi_{jk}(x) = 2^{-j/2} \sum_{m_j=2^j}^{2^{j+1}-1} \mathrm{e}^{2\pi \mathrm{i} m_j (x-\frac{k}{2^j})}, \tag{1}$$

and an associated orthonormal harmonic wavelet basis

$$B_n = \{\phi, \psi_{jk}, \psi^*_{jk}, \psi_{n-1}\}_{j=0,1,\ldots,n-2;\ k=0,1,\ldots,2^j-1}, \tag{2}$$

where $(\cdot)^*$ denotes complex conjugation, ϕ (the father wavelet) is defined as 1, and ψ_{n-1} is the highest resolved frequency:

$$\psi_{n-1} = \mathrm{e}^{-\frac{N}{2} 2\pi \mathrm{i} x}. \tag{3}$$

In this formulation, the harmonic wavelet space $W_n = span\{B_n\}$ coincides with the usual Fourier space spanned by the same number of basis elements, with wave numbers from $-N/2$ to $N/2-1$. Actually, the space generated by the wavelets at the same level (or scale) j is spanned by a block of contiguous Fourier modes. This fact allows for a fast wavelet transform, based on fast Fourier transforms (FFTs) on the corresponding levels [6].

The projection of any real-valued function $u(x) \in L^2([0, 1])$ onto W_n is given by

$$u_N(x) = a_0 + \sum_{j=0}^{n-2} \sum_{k=0}^{2^j-1} (a_{j,k}\psi_{j,k}(x) + a^*_{j,k}\psi^*_{j,k}(x)) + a_{N/2}\psi_{n-1}(x), \tag{4}$$

where $N = 2^n$ and the harmonic wavelet coefficients $a_{(\cdot)}$ are obtained from the Fourier coefficients, independently on each scale level j, through FFTs of length 2^j.

We now consider the nonlinear 1D Burgers equation, with diffusion

$$D(u(x,t)) = \frac{\partial u(x,t)}{\partial t} + u(x,t)\frac{\partial u(x,t)}{\partial x} - \nu \frac{\partial^2 u(x,t)}{\partial x^2} = 0, \quad x \in (0,1). \tag{5}$$

The harmonic wavelet Galerkin method for this equation is obtained by considering an expansion of the solution u in the space W_n, with time-dependent coefficients. Imposing that $\langle Du, v\rangle = 0$ for any $v \in W_n$ leads to the following system of differential equations for the coefficients of the expansion of u (in the form (4)):

$$\begin{aligned}
&\frac{\mathrm{d}\, a_0(t)}{\mathrm{d}t} = 0\\
&\frac{\mathrm{d}\, a_{r,s}(t)}{\mathrm{d}t} = -a_0(t) \sum_{q=0}^{2^r-1} a_{r,q}(t)\gamma^r_{qs} - \sum_{j,p=0}^{n-2} \sum_{k=0}^{2^j-1} \sum_{q=0}^{2^p-1} (a_{j,k}(t)a_{p,q}(t)P(0)^{jpr}_{kqs} + a^*_{j,k}(t)a_{p,q}(t)P(1)^{jpr}_{kqs})\\
&\qquad - \sum_{j,p=0}^{n-2} \sum_{k=0}^{2^j-1} \sum_{q=0}^{2^p-1} (a_{j,k}(t)a^*_{p,q}(t)P(2)^{jpr}_{kqs}) + \nu \sum_{k=0}^{2^r-1} a_{r,k}(t)\, \chi^r_{ks}\\
&\qquad \text{for } r = 0, 1, \ldots, n-2, \quad s = 0, 1, \ldots, 2^r - 1,\\
&\frac{\mathrm{d}\, a_{N/2}(t)}{\mathrm{d}t} = N\pi \mathrm{i}\, a_0(t)a_{N/2}(t) - \sum_{j,p=0}^{n-2} \sum_{k=0}^{2^j-1} \sum_{q=0}^{2^p-1} (a^*_{j,k}(t)a^*_{p,q}(t)N^{jp*}_{kq}) - \nu\,(N\pi)^2 a_{N/2}(t),
\end{aligned} \tag{6}$$

where

$$\begin{aligned}
\gamma^r_{ks} &= \left\langle \frac{\mathrm{d}\, \psi_{r,k}(x)}{\mathrm{d}x}, \psi_{r,s}(x) \right\rangle\\
&= 2\pi \mathrm{i}\, 2^{-r} \sum_{w=2^r}^{2^{r+1}-1} w \mathrm{e}^{-2\pi \mathrm{i} w \frac{k-s}{2^r}}
\end{aligned} \tag{7}$$

are first-order linear connection coefficients and

$$\chi^r_{ks} = \left\langle \frac{\mathrm{d}^2\psi_{r,k}(x)}{\mathrm{d}x^2}, \psi_{r,s}(x) \right\rangle = -4\pi^2\, 2^{-r} \sum_{w=2^r}^{2^{r+1}-1} w^2 \mathrm{e}^{-2\pi \mathrm{i} w \frac{k-s}{2^r}} \tag{8}$$

are second-order linear connection coefficients. The nonlinear connection coefficients are given by

$$P(0)^{jpr}_{kqs} = \left\langle \psi_{j,k}(x) \frac{\mathrm{d}\,\psi_{p,q}(x)}{\mathrm{d}x}, \psi_{r,s}(x) \right\rangle = \frac{2\pi\,\mathrm{i}}{2^{(j+p+r)/2}} \sum_{m_j=2^j}^{2^{j+1}-1} \sum_{m_p=n_1(r,p,m_j)}^{n_2(r,p,m_j)} m_p \mathrm{e}^{-2\pi\mathrm{i}\left(\frac{m_j k}{2^j} + \frac{m_p q}{2^p} - \frac{(m_j+m_p)s}{2^r}\right)}, \tag{9}$$

$$P(1)^{jpr}_{kqs} = \left\langle \psi^*_{j,k}(x) \frac{\mathrm{d}\,\psi_{p,q}(x)}{\mathrm{d}x}, \psi_{r,s}(x) \right\rangle = \frac{2\pi\,\mathrm{i}}{2^{(j+p+r)/2}} \sum_{m_j=2^j}^{2^{j+1}-1} \sum_{m_p=n_1(r,p,-m_j)}^{n_2(r,p,-m_j)} m_p \mathrm{e}^{-2\pi\mathrm{i}\left(-\frac{m_j k}{2^j} + \frac{m_p q}{2^p} - \frac{(m_p-m_j)s}{2^r}\right)}, \tag{10}$$

$$P(2)^{jpr}_{kqs} = \left\langle \psi_{j,k}(x) \frac{\mathrm{d}\,\psi^*_{p,q}(x)}{\mathrm{d}x}, \psi_{r,s}(x) \right\rangle = (P(0)^{rpj}_{sqk})^* \tag{11}$$

$$N^{jp}_{kq} = \left\langle \psi^*_{j,k}(x) \frac{\mathrm{d}\,\psi^*_{p,q}(x)}{\mathrm{d}x}, \psi_{n-1}(x) \right\rangle = \frac{2\pi\,\mathrm{i}}{2^{(j+p)/2}} \sum_{m_p=\max(N/2-(2^{j+1}-1),2^p)}^{\min(N/2-2^j,2^{p+1}-1)} m_p \mathrm{e}^{2\pi\mathrm{i} m_p\left(\frac{k}{2^j} - \frac{q}{2^p}\right)}. \tag{12}$$

In the expressions for $P(0)$ and $P(1)$, we have $n_1(r, p, m_j) = \max(2^r - m_j, 2^p)$ and $n_2(r, p, m_j) = \min(2^{r+1} - 1 - m_j, 2^{p+1} - 1)$. All these connection coefficients can be precomputed, since they only depend on the basis elements.

For the solution of system (6) we may employ any ordinary differential equation (ODE) solver. We consider explicit schemes in our complexity estimates. The computationally dominant part in the evaluation of the right-hand side (RHS) of this system is the projection of the nonlinear term uu_x onto each basis element. For every pair (r, s), $r = 0, \ldots, n-2$, $s = 0, \ldots, 2^r - 1$, there are $O(N^2)$ terms in the sums involving the nonlinear connection coefficients. For a scale triad j, p, r, only scales j, p that are smaller or equal to r give rise to non-zero connection coefficients $P(0)^{jpr}_{kqs}$ (similar results hold for the other nonlinear coefficients). However, we have $2^{n-2} = O(N)$ pairs (r, s) with $r = n-2$. For those, we have $O(N^2)$ non-zero connection coefficients. Therefore, the computational work to evaluate the RHS of system (6) amounts to $O(N^3)$.

2.1. Algorithmic variants

In Fig. 1, we display the coefficients $P(0)^{jpr}_{kqs}$ graphically for some pairs (r, s) (for $n = 5$) at the finer scales ($r = 3$). In the bottom line of the figure, we can observe, with the help of a logarithmic scale, that the matrix of coefficients gets practically full. In the top line, we present the same matrices with a linear scale, and we see that many of them are close to zero. This is due to the localization properties of the harmonic wavelets. Although not having a compact support, they are locally concentrated. For a wavelet $\psi_{r,s}(x)$, we associate intervals

$$I^d_{r,s} = \left[\frac{s-d}{2^r}, \frac{s+d}{2^r}\right], \quad d = 1, 2, \ldots$$

(with natural periodic extensions if $s/2^r$ is close to the border of $[0, 1]$). We have that the L^2 norm of $\psi_{r,s}(x)$ in $I^d_{r,s}$ is about 90% of its norm in the full interval $[0, 1]$ for $d = 1$, reaching respectively close to 95% and 97% for $d = 2$ and $d = 3$. The same is true for the first derivative of $\psi_{r,s}(x)$. This motivates the first algorithmic simplification in the Galerkin scheme. The connection coefficients, linear and nonlinear, are set to zero if

$$I^d_{r,s} \cap I^d_{j,k} = \emptyset \quad \text{or} \quad I^d_{r,s} \cap I^d_{p,q} = \emptyset.$$

for a fixed (small) value of d. This use of the wavelet localization properties was employed in [7], but only for $d = 1$.

We now deduce the computational complexity per time step when we employ a fixed value of $d > 0$ in this simplified scheme. Each wavelet $\psi_{r,s}(x)$ will lead to non-zero nonlinear coefficients when it interacts in a triad with lower levels $j \le r$,

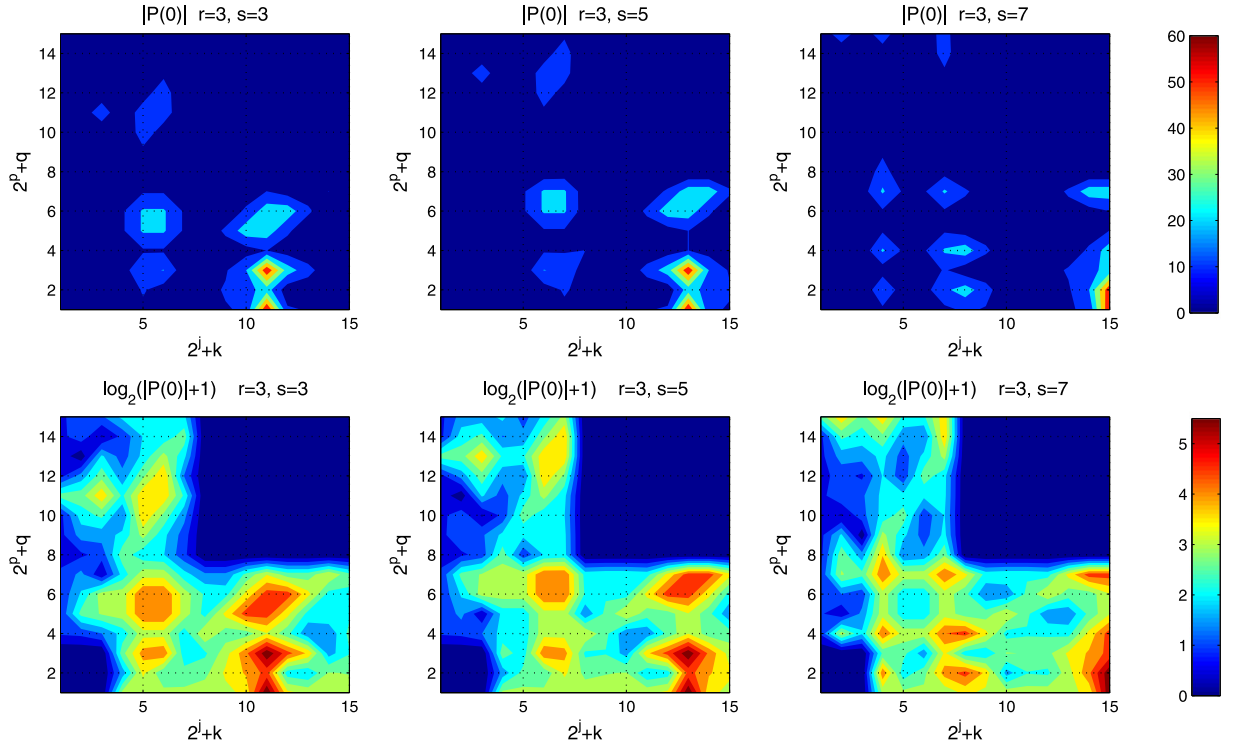

Fig. 1. Absolute values of the nonlinear connection coefficients $P(0)^{ipr}_{kqs}$ for some pairs (r, s) at the finest scale (for $n = 5$). In the top line we use a linear scale; in the bottom line the same values are displayed in logarithmic scale. In each individual figure, the matrix of coefficients for a fixed pair (r, s) is shown, with $2^j + k$ varying in the horizontal axis and $2^p + q$ in the vertical.

$p \le r$. At each level, $I^d_{r,s}$ will have a non-empty intersection with $2d$ or $2d + 1$ intervals. Taking into account that at each level r we have 2^r wavelets (for $s = 0, \ldots, 2^r - 1$), we conclude that the total number of non-zero nonlinear coefficients is limited by

$$\begin{aligned} T &= \sum_{r=0}^{n-2} 2^r (r+1)^2 (2d+1)^2 = (2d+1)^2 \sum_{r=0}^{n-2} 2^r (r^2 + 2r + 1) \\ &= (2d+1)^2 \left(\sum_{r=0}^{n-2} r^2 2^r + 2 \sum_{r=0}^{n-2} r 2^r + \sum_{r=0}^{n-2} 2^r \right). \end{aligned} \tag{13}$$

Expanding the sum

$$\begin{aligned} \sum_{r=0}^{n-2} r^2 2^r &= (2 + 2^2 2^2 + 3^2 2^3 + \cdots + (n-2)^2 2^{n-2}) \\ &= (2 + 2^2 + \cdots + 2^{n-2}) + 3(2^2 + 2^3 + \cdots + 2^{n-2}) + \cdots + (2n-5)2^{n-2} \\ &= (2^{n-1} - 2) + 3(2^{n-1} - 2^2) + \cdots + (2n-5)(2^{n-1} - 2^{n-2}) \\ &= 2^{n-1}(1 + 3 + \cdots + (2n-5)) - (1 \times 2 + 3 \times 2^2 + \cdots + (2n-5)2^{n-2}) \\ &= 2^{n-1}(n-2)^2 - \sum_{r=1}^{n-2} (2r-1)2^r \\ &= 2^{n-1}(n-2)^2 - 2 \sum_{r=1}^{n-2} r 2^r + (2^{n-1} - 2) \end{aligned}$$

and using this last expression in (13), we get

$$\begin{aligned} T &= (2d+1)^2 (2^{n-1}(n-2)^2 + (2^{n-1} - 2) + (2^{n-1} - 1)) \\ &= (2d+1)^2 (2^{n-1}((n-2)^2 + 2) - 3) \\ &= O(2^n n^2) = O(N(\log N)^2), \end{aligned}$$

Table 1
Computational costs of several variants of the wavelet Galerkin method.

Algorithmic variant	Comp. complexity
Harm. wav. – full connection coefficients	$O(N^3)$
Harm. wav. – frequency restrictions ($d = 0, \xi > 0$)	$O(N^3)$
Harm. wav. – support restrictions ($d > 0, \xi = 0$)	$O(N(\log N)^2)$
Harm. wav. – freq. and supp. restric. ($d > 0, \xi > 0$)	$O(N)$
Harm. wav. – pseudo-spectral	$O(N \log N)$

establishing the computational complexity of this simplified variant of the Galerkin scheme. We notice that the projection of the linear part, associated to the diffusion term, amounts to $O(N^2)$ operations if we do not restrict the support interactions. In the simplified version, with $d > 0$, these costs are reduced to $O(N)$. The overall complexity will be of $O(N(\log N)^2)$.

Another assumption used in [7] is to consider that interactions between neighboring scales are the relevant ones. They proposed to neglect the nonlinear connection coefficients related to the triads $\{j, p, r\}$ if $|r - j| > 1$ or $|r - p| > 1$, retaining only the coefficients associated to triads of the form $\{r - 1, r - 1, r\}$, $\{r - 1, r, r\}$ or $\{r, r - 1, r\}$. We extend this variation, considering the possibility of neglecting interactions only if their scales are more than ξ levels apart, for a parameter $\xi \geq 1$ (with $\xi = 1$ corresponding to the modification in [7]). In this variant, we consider the nonlinear connection coefficients from triads $\{j, p, r\}$ to be zero if $|r - j| > \xi$ or $|r - p| > \xi$. We can actually combine both simplifications, exploiting the localization properties (through the parameter d) and restricting the scale interactions (through the parameter ξ). With the understanding that $d = 0$ means no restriction in the wavelet supports and $\xi = 0$ means no restriction in the scale interaction, we have through the combinations of these parameters several variants of the wavelet Galerkin method, with the pair $d = 0, \xi = 0$ corresponding to the unmodified harmonic wavelet Galerkin scheme. We now derive the computational complexity of these combinations. We first observe that, if we restrict the scale interaction (with $\xi = 1$ for example) but still employ the full support of the wavelets (with $d = 0$), the resulting scheme still presents $O(N^3)$ complexity per time step. Notice that to each triad of the form $\{n - 2, n - 3, n - 2\}$ or $\{n - 3, n - 2, n - 2\}$ there correspond $O(N^2)$ non-zero connection coefficients, and since there are $O(N)$ of them, the high complexity follows. On the other hand, if we take $d > 0$, the restriction in scale interaction ($\xi > 0$) will change the computational complexity in the following way. In the expression for the upper bound T in (13), the value $(r + 1)^2$ will become $(\xi + 1)^2$, independent of r. In this way, the total number of non-zero nonlinear coefficients will be reduced to

$$\begin{aligned} T &= \sum_{r=0}^{n-2} 2^r (\xi + 1)^2 (2d + 1)^2 = (\xi + 1)^2 (2d + 1)^2 \sum_{r=0}^{n-2} 2^r \\ &= (\xi + 1)^2 (2d + 1)^2 2^{n-1} = O(N), \end{aligned}$$

showing that this variant presents optimal complexity, with only $O(N)$ operations per time step.

2.2. Pseudo-spectral method

As an alternative, consider a pseudo-spectral [12] formulation for the wavelet Galerkin method. Instead of working with the nonlinear connection coefficients, an auxiliary grid is introduced in order to evaluate the projection of the product uu_x. The idea is to evaluate the function u and its derivative u_x on the uniform mesh formed by the points $x_j, j = 1, \ldots, M$, with $x_j = j/M$. If we choose $M = N$, we have a one to one correspondence between the function coefficients and the function grid values. Having u and u_x on the mesh, we can easily form the product, and from its values on the mesh get the wavelet coefficients of uu_x. In order to get the function values on the mesh, we first transform the wavelet coefficients of u to Fourier coefficients (using FFTs, one for each scale). From the Fourier coefficients we easily derive the Fourier coefficients of u_x, and through FFTs we evaluate both functions on the grid. Once the product is built, another FFT generates the Fourier coefficients. From those, the wavelet coefficients of the product are obtained through another set of FFTs, one on each scale. Using $M = N$ will lead to aliasing of high frequencies onto lower ones, since the product will have more Fourier modes than the individual functions. Setting $M = 3N/2$ is enough to obtain the coefficients of uu_x alias free (see [13]). The wavelet transforms, from wavelet coefficients to Fourier coefficients and vice versa, as well as the direct and inverse Fourier transforms between the grid and Fourier coefficients, amount to a total of $O(N \log N)$ operations. The evaluation of the coefficients of the linear diffusion term can either be obtained via the Fourier coefficients of u, from which one easily derives the Fourier coefficients of u_{xx} and transform to wavelet space, or through the linear connection coefficients χ^r_{ks}. This latter version implies $O(N^2)$ operations, against the $O(N \log N)$ from the transforms. If one uses the support restriction (with $d > 0$) for the linear connection coefficients, then this part of the algorithm only amounts to $O(N)$ operations. We can therefore have the pseudo-spectral wavelet scheme with a total of $O(N \log N)$ operations per time step of the ODE solver (this is the same complexity as that of a pseudo-spectral Fourier method).

We summarize the computational complexity of the several algorithmic variants of the wavelet Galerkin scheme in Table 1.

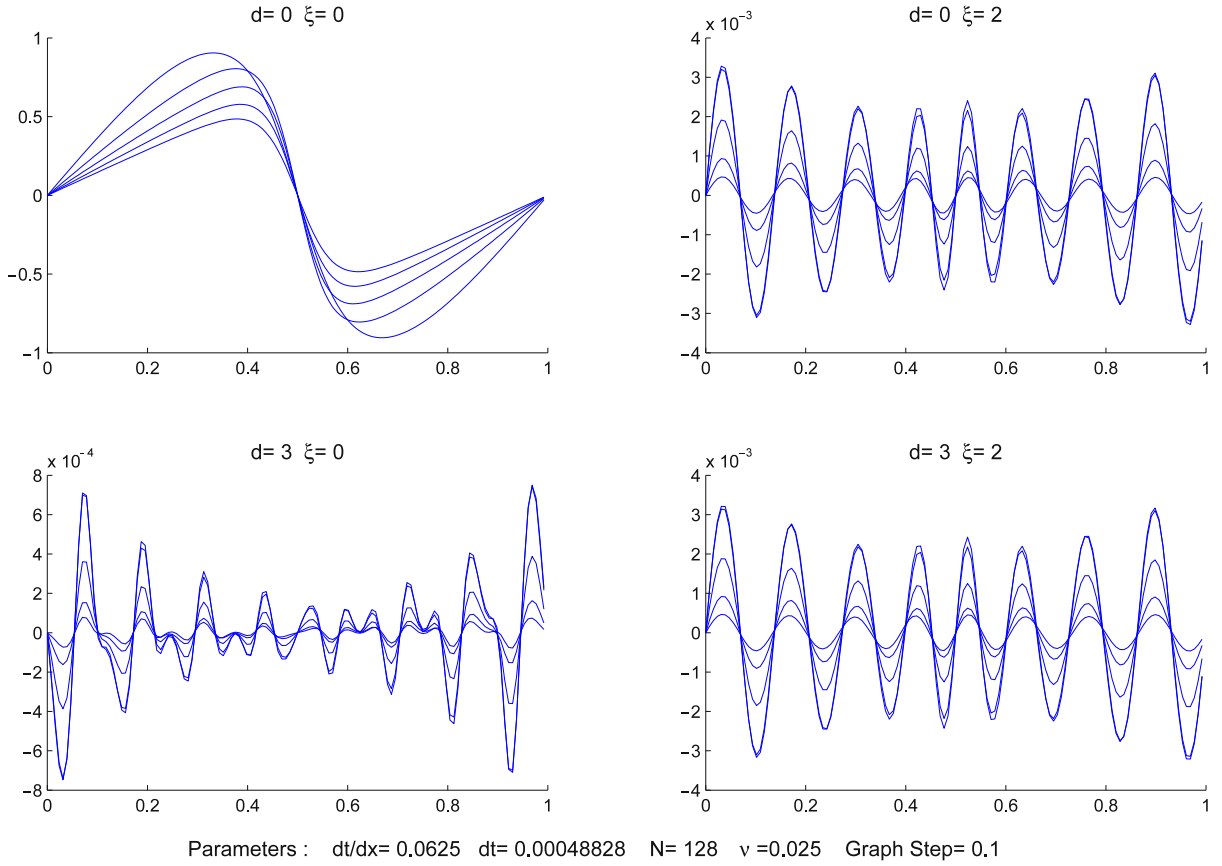

Fig. 2. Harmonic wavelet numerical solution of the Burgers equation with $N = 128$, $\mathrm{d}t = \frac{1}{16N}$, with graphics at every 0.1 instant of time. The results with the full connection coefficients ($d = 0, \xi = 0$) are shown on the top, left. The other graphics show errors in relation to this solution, obtained with the other variants.

3. Numerical experiments

We started the comparative tests of the several variants of the wavelet Galerkin method with an example used in [7]. We set $u(x) = \sin 2\pi x$ as the initial state and use $\nu = 0.025$. We employ a forth-order Runge–Kutta scheme to advance the computations in time, in order to keep the time discretization errors small, so we can access better the effects of the different treatments in space. In Fig. 2, we compare the results of a time integration up to time instant 0.5, obtained with the wavelet Galerkin scheme for some choice of the parameters d and ξ. We observe that the simplified versions, with restrictions in the support interactions ($d = 3$) and or frequencies ($\xi = 2$), produce results similar to the ones obtained with the scheme with the full connection coefficients ($d = 0$ and $\xi = 0$), although introducing some growing noise. The errors reach the order of 7×10^{-4} with $d = 3$ and $\xi = 0$ and of order of 3×10^{-3} with $\xi = 2$ and $d = 0$ or $d = 3$.

In Fig. 3, we explore more combinations of the cutting parameters ξ and d, employing as the initial state a more localized function (defined as $u(x) = 0.5 + \mathrm{e}^{-10^{-5}(x-0.3)^4}$). The effects of the simplifications on the numerical solutions obtained become more accentuated. Clearly, frequency cuts can significantly modify the form of the signal, and restricting the interactions of the supports with $d = 1$ introduces unacceptable errors. With $d = 3$ and $\xi = 0$, the results get closer to the ones with the full scheme ($d = 0, \xi = 0$), with errors of the order of 1%. More extensive tests can be found in [14].

4. Simulation of precipation fronts

In this section, we consider the applicability of the harmonic wavelet Galerkin method to a simple (non-dimensional) meteorological model. It consists of a precipitation front propagation model for the tropical atmosphere, developed in [10], which represents well the precipitation phenomenon near the equator. We consider here the barotropic only version of the

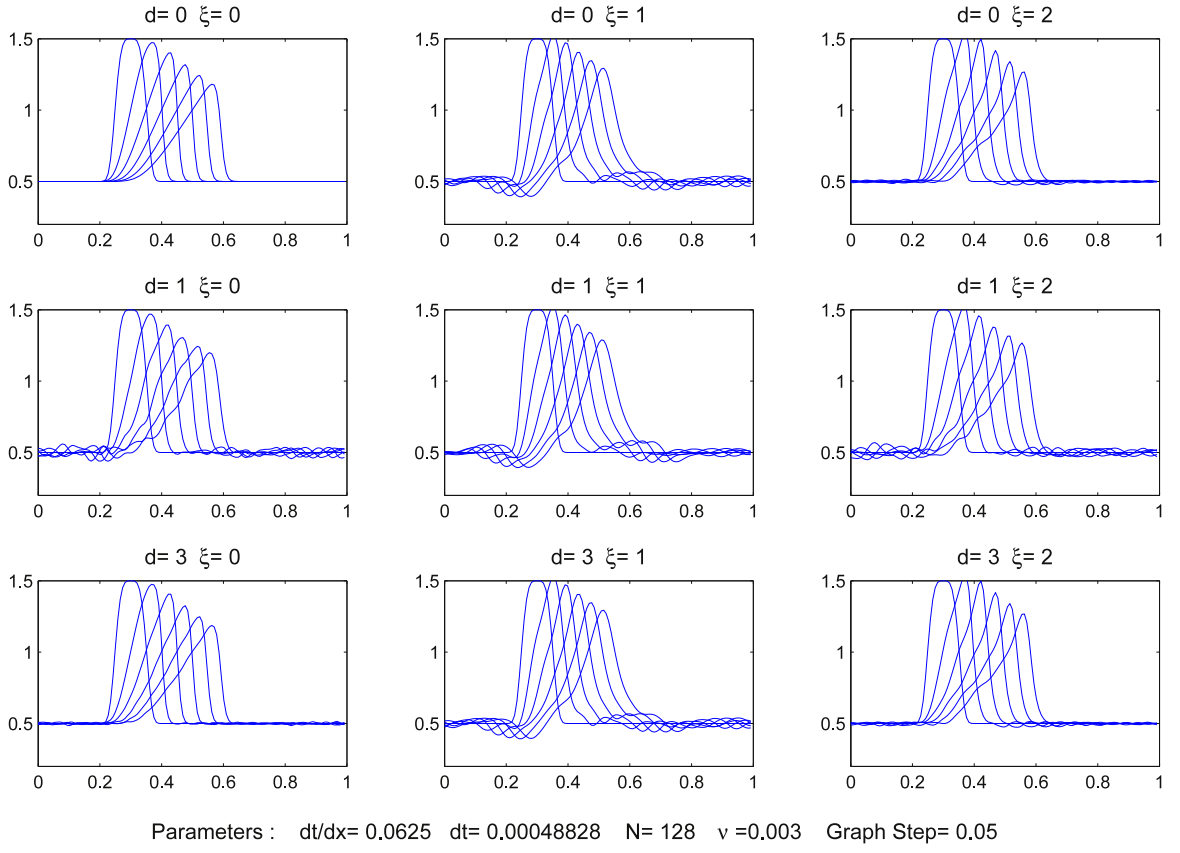

Fig. 3. Harmonic wavelet numerical solution of the Burgers equation using $N = 64$, $\mathrm{d}t = \frac{1}{16N}$, with a pulse as the initial state. Results at every 0.05 time unit are shown for several variants.

model, given by

$$\begin{aligned} \frac{\partial u}{\partial t} &= \frac{\partial T}{\partial x} \\ \frac{\partial T}{\partial t} &= \frac{\partial u}{\partial x} + P \\ \frac{\partial q}{\partial t} &= -Q\frac{\partial u}{\partial x} - P. \end{aligned} \tag{14}$$

Here, u is the zonal wind speed, T is the perturbation around a basic state temperature, P is the precipitation field, q the humidity level, and Q parameterizes the gross moisture stratification. The precipitation field is given as a (nonlinear) function of temperature and humidity as $P = \frac{1}{\tau}(q - \tilde{q}(T))^+$, where $(a)^+ = \{a, \text{if } a > 0;\ 0 \text{ otherwise}\}$. Precipitation occurs only when the humidity gets above $\tilde{q}(T)$, a prescribed function of temperature. The parameter τ is a convective adjustment time. In our tests, we adopt $\tilde{q}(T) = \hat{q} + \alpha T$, where $\hat{q}$ is an average value for moisture saturation and α is a constant in $(0, 1)$.

Although simple, this model provides good insights about precipation fronts in the tropical region [10]. From continuous initial conditions, with discontinuities in the first derivatives, sharp precipation fronts can be formed. Therefore, this model is adequate to test the wavelet Galerkin method and its localization properties. In our tests, we use the following parameters: $Q = 0.9$, $\hat{q} = 0.9$, $\alpha = 0.6$ and $\tau = 0.00625$. The initial fields are set as $u(x) = 0.01|x - 0.5|$, $T = 0.0073\,(0.5 - |x - 0.5|)$, $q = \hat{q} + \alpha T$ and $P = 0$. These initial conditions were chosen according to considerations in [15,16], in order to produce what is called a dying front, which consists of a moistening front propagating eastwards, followed by a faster drying front in the same direction.

The wavelet Galerkin scheme follows the same lines of the method described in Section 2. We consider (time-dependent) expansions of the four variables (as in Eq. (4)) in the space of harmonic wavelets W_n, use them in system (14) and require the residuals of the equations to be orthogonal to each basis element of W_n. This leads to a system of ODEs for the wavelet coefficients of u, q, T and P, which are coupled in each scale level by the linear connection coefficients γ^r_{ks} defined in (7). However, P depends nonlinearly on q and T. In order to obtain the wavelet coefficients of P, we first use fast wavelet transforms to obtain the values of the humidity and temperature on the uniform grid in

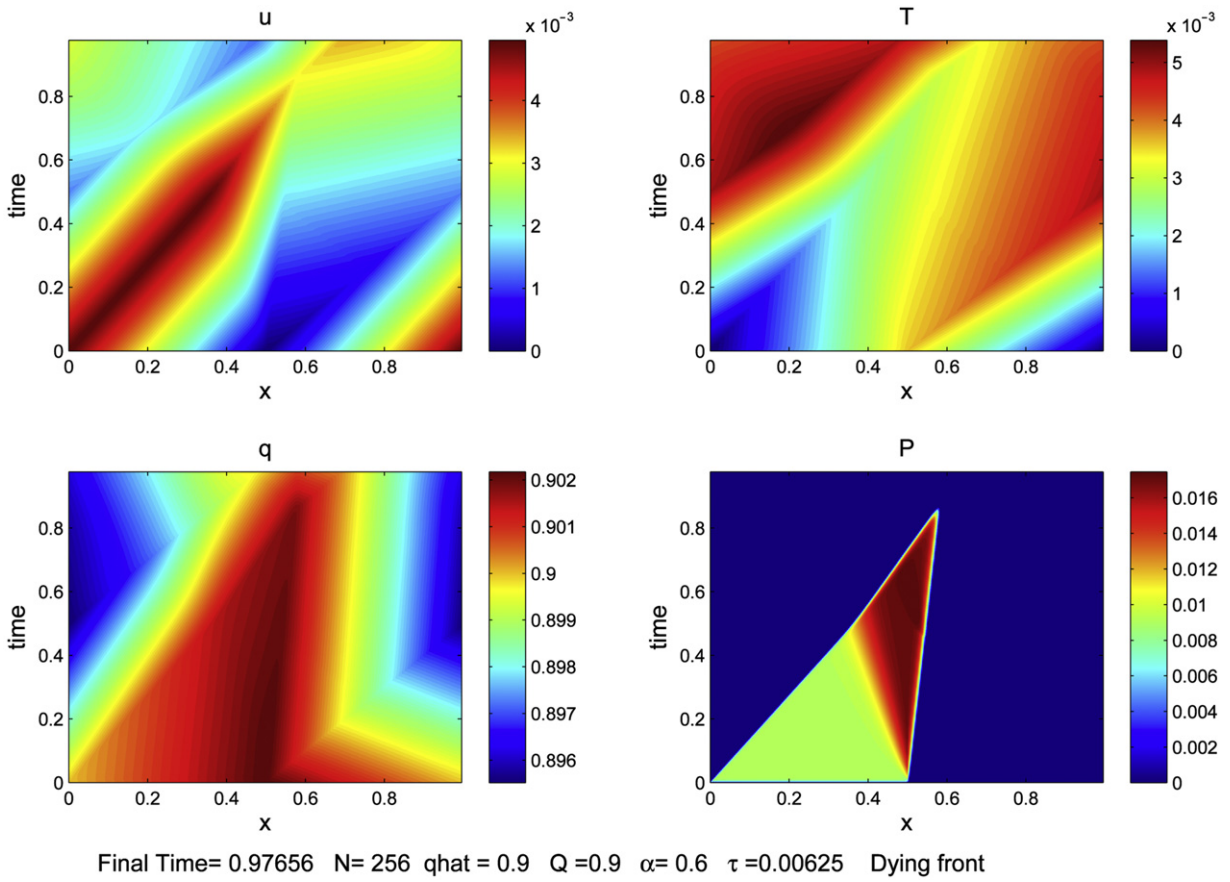

Fig. 4. Time evolution of the fields u, T, q and P in the simulation of a dying front with the full wavelet Galerkin method, with $N = 256$ and $dt = \frac{1}{16N}$.

$[0, 1]$, with grid spacing $1/N$. The precipitation field is then evaluated, and its wavelet coefficients are obtained through another wavelet transform. This scheme amounts to $O(N^2)$ operations to evaluate the RHS of the system, due to the coupling of the coefficients at the same scale. The calculation of the coefficients of P is done in $O(N \log N)$ operations with the fast transforms. The total computational complexity of the method is $O(N^2)$ per time step. It can be reduced to $O(N \log N)$ by employing the restrictions in support (with $d > 0$) in the computation of the linear connection coefficients. Alternatively, we could use a pure pseudo-spectral method, applying the wavelet transforms also in the evaluation of the coefficients of the x-derivatives of the fields. The pseudo-spectral formulation also amounts to $O(N \log N)$ operations per time step, but with the advantage of no loss in precision in relation to the scheme with the full connection coefficients ($d = 0$).

In Fig. 4, we display the time evolution of the fields u, T, q and P. We can observe that we get precipitation in the first half of the domain immediately after the start of the simulation, since the humidity has been initialized with $q = \tilde{q}(T)$ in our initial condition. Notice that, at the initial state, $\partial u/\partial x$ is negative for $x \in [0, 0.5]$ and positive at the second half of the domain. This causes the humidity to increase in $[0, 0.5]$, causing the precipitation to start. The wet region moves right with a moistening front moving at an approximate (nondimensional) speed of 0.09. At the same time, we observe that the wet region is diminishing in size, with the drying front moving much faster. When this latter front reaches the moistening one, the precipitation dies out, at around 0.85 time units of simulation. Snapshots of the precipitation field at given time instants are shown in Fig. 5, together with its wavelet coefficients at the finest level (the coefficient of $\psi_{j,k}(x)$ is plotted at the point $k/2^j$). From the coefficients we can clearly see the front locations and their evolution.

In Fig. 6, we compare the precipitation field at instant 0.3 obtained with the Galerkin scheme using the support restriction parameter $d = 0$, $d = 1$ and $d = 3$ (a forth-order Runge–Kutta ODE solver has been used in all cases). We notice that the results with $d = 1$ are rather noisy (although the location and intensity of the precipitation is captured). With $d = 3$ some noise remains, but the result is much closer to the one obtained with the (full) method with no restrictions ($d = 0$). The pseudo-spectral method leads to the same results as with $d = 0$ with better computational efficiency. Finally, at the same instant, we display in Fig. 7 the wavelet coefficients of the precipitation field at the three finest levels. We observe that the localization of the fronts (compare with Fig. 6) has already been captured at level 5. The extra levels will normally

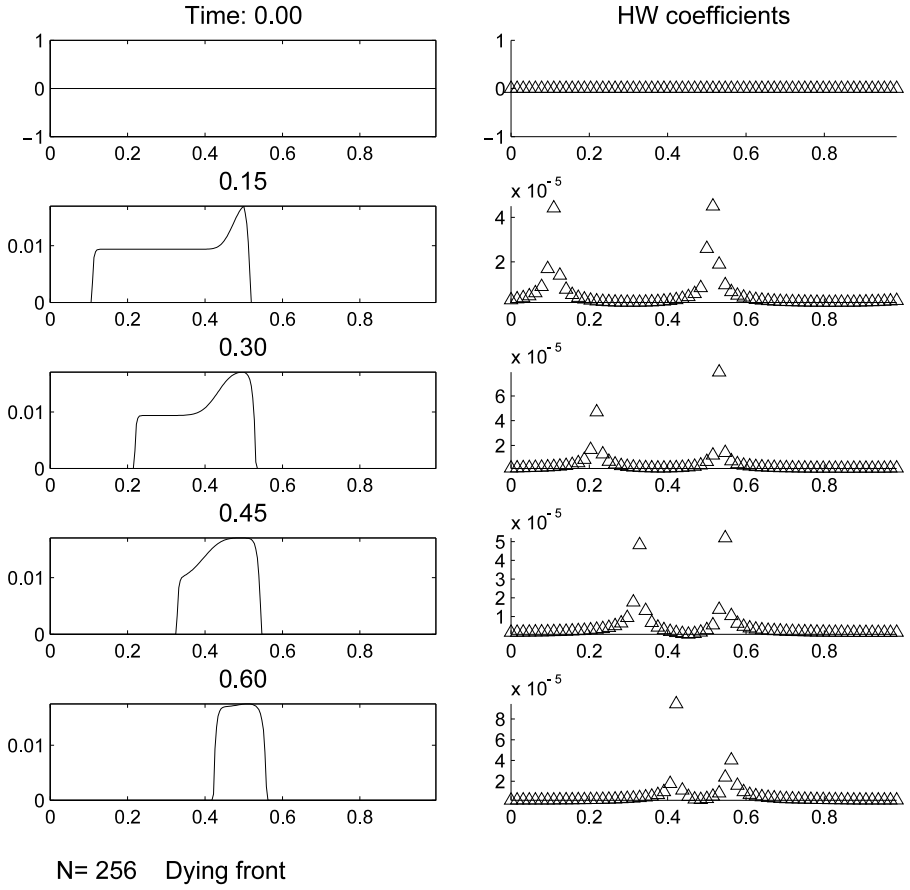

Fig. 5. Snapshots of the precipitation field and its finest level wavelet coefficients at given time instants of the dying front simulation of Fig. 4.

improve the resolution of this localization, with the position of the highest coefficients at each level converging to the front locations.

5. Conclusions

We have experimented with different formulations of a harmonic wavelet Galerkin method, using the nonlinear Burgers equation as a model test. We considered a spectral formulation based on linear and nonlinear connection coefficients. Although allowing for an explicit analytic derivation of the connection coefficients, this formulation is very costly, with a computational complexity of order $O(N^3)$ per time step, where N is the dimension of the wavelet space. Variants of this formulation, exploiting the locality of the wavelets and ideas of restricting the scale interactions when computing the connection coefficients, have been analyzed, in a more general way than proposed in [7]. The resulting simplified schemes present computational complexities that can be reduced even to $O(N)$. However, neglecting scale interactions between non-neighboring levels has shown a negative impact on the accuracy of computations and does not seem to pay off. Restrictions of support may be used with care, leading to acceptable results if we do not restrict the supports to a too narrow interval. This will lead to schemes with $O(N(\log N))^2$ complexity. These schemes were also compared to a pseudo-spectral formulation of the wavelet Galerkin method. Making use of a fast wavelet transform, based on FFTs, this method achieves a suboptimal complexity of $O(N \log N)$, with no degradation in accuracy when compared to the version based on the full set of connection coefficients.

The schemes have been efficiently applied to a simple nonlinear meteorological model for simulating the propagation of precipitation fronts. The numerical results show that the front locations are very well described by the intensity of the wavelet coefficients. These results indicate that, in spite of the fact that harmonic wavelets decay somewhat slowly, it may be feasible to exploit their locality, selecting the more relevant local basis elements in the wavelet expansions, but this remains to be investigated. The restriction in support when computing the connection coefficients, with appropriate choice of parameters, makes a possible alternative for an efficient method, but with some loss in precision. The pseudo-spectral version is the most interesting for this nonlinear model for precipitation fronts.

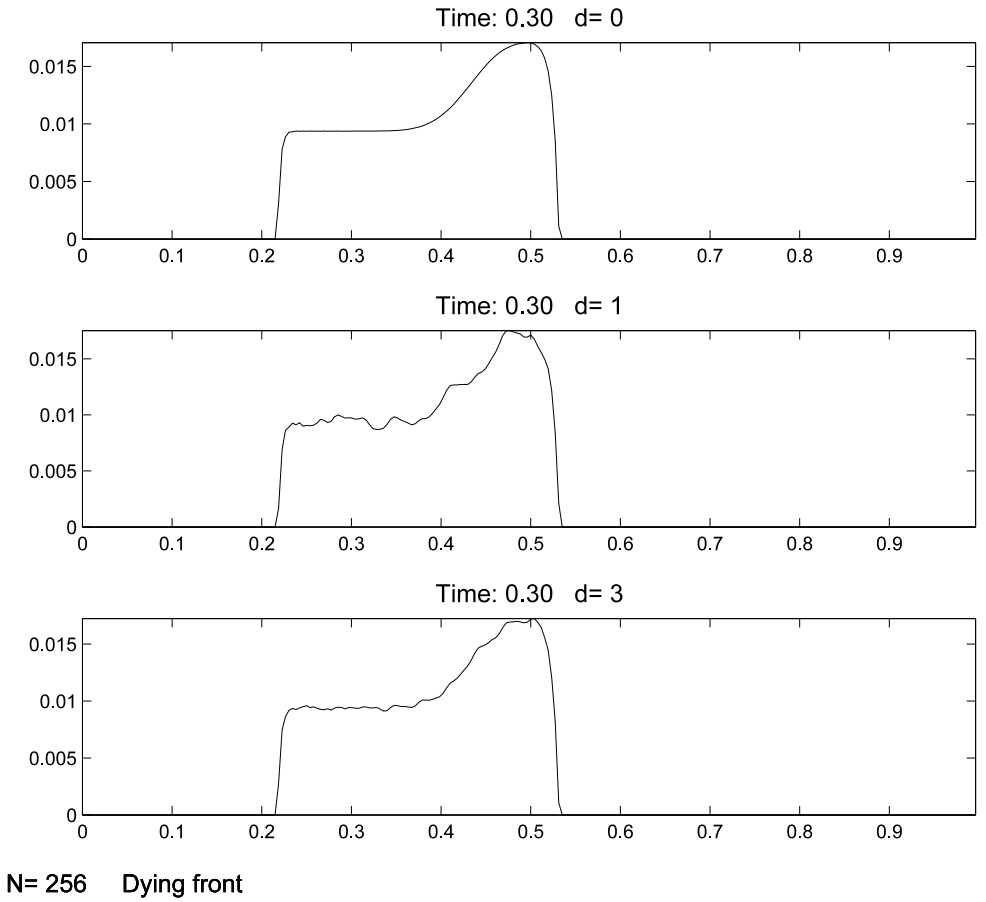

Fig. 6. Precipitation field at instant 0.3 calculated with parameters $d = 0$, $d = 1$ and $d = 3$ in the wavelet Galerkin method.

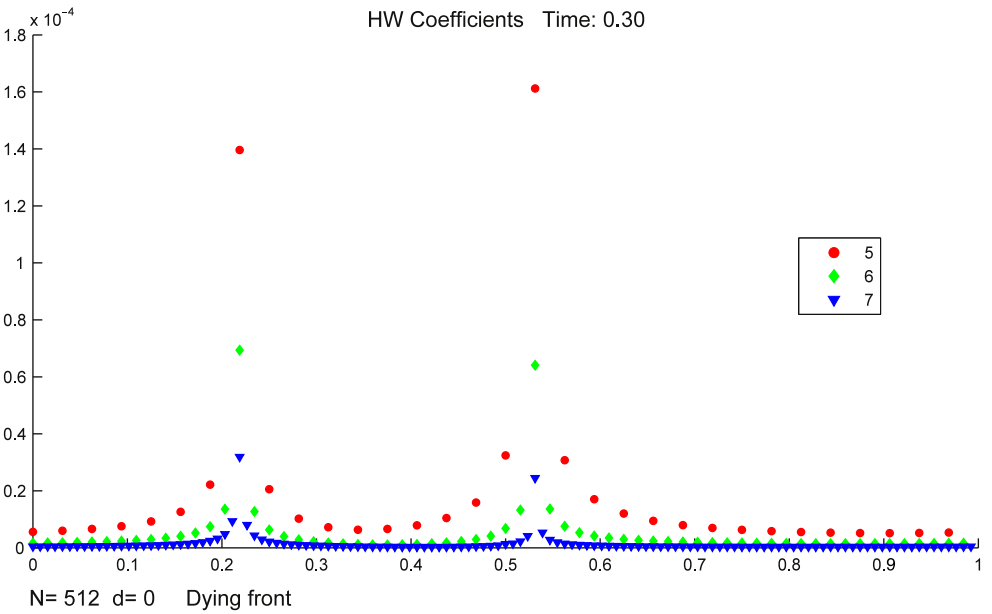

Fig. 7. Wavelet coefficients of the precipitation field at instant 0.3. Only the three finest levels are shown. Simulations were done with $N = 512$ and the full wavelet Galerkin method.

Acknowledgements

We are grateful to Juliana Faus da Silva Dias for bringing the precipation front propagation model to our attention and to Carlo Cattani for interesting discussions. Pedro S. Peixoto is grateful for support from CNPq.

References

[1] S.L. Ho, S.Y. Yang, Wavelet-Galerkin method for solving parabolic equations in finite domains, Finite Elem. Anal. Des. 37 (2001) 1023–1037.
[2] E.B. Lin, X. Zhou, Connection coefficients on an interval and wavelet solutions of Burgers equation, J. Comput. Appl. Math. 135 (2001) 63–78.
[3] R.L. Schult, H.W. Wyld, Using wavelets to solve the Burgers equation: a comparative study, Phys. Rev. A 46 (1992) 7953–7958.
[4] M.O. Domingues, S.M. Gomes, O. Roussel, K. Schneider, An adaptive multiresolution scheme with local time stepping for evolutionary PDEs, J. Comput. Phys. 227 (2008) 3758–3780.
[5] K. Schneider, M. Farge, Numerical simulation of the transient flow behaviour in tube bundles using a volume penalization method, J. Fluids Struct. 20 (2005) 555–566.
[6] D. Newland, Harmonic wavelet analysis, Proc. R. Soc. Lond. A 443 (1993) 203–225.
[7] S.V. Muniandy, I.M. Moroz, Galerkin modelling of the Burgers equation using harmonic wavelets, Phys. Lett. A 235 (1997) 352–356.
[8] C. Cattani, Harmonic wavelets towards the solution of nonlinear PDE, Comput. Math. Appl. 50 (2005) 1191–1210.
[9] C. Cattani, Harmonic wavelet solution of Poisson's problem, Balkan J. Geom. Appl. 13 (2008) 27–37.
[10] D.M.W. Frierson, A.J. Majda, O.M. Pauluis, Large scale dynamics of precipitation fronts in the tropical atmosphere: a novel relaxation limit, Commun. Math. Sci. 2 (2004) 591–626.
[11] I. Daubechies, Ten Lectures on Wavelets, SIAM, Philadelphia, 1992.
[12] D. Gottlieb, S.A. Orzag, Numerical Analysis of Spectral Methods: Theory and Applications, SIAM, Philadelphia, 1977.
[13] C. Canuto, M.Y. Hussaini, A. Quarteroni, T.A. Zang, Spectral Methods in Fluid Dynamics, Springer, New York, 1988.
[14] P.S. Peixoto, Resolução numérica de EDPs utilizando ondaletas harmônicas, master thesis, IME — Universidade de São Paulo 2009, available in http://www.teses.usp.br/teses/disponiveis/45/45132/tde-02082009-192253/ (in portuguese).
[15] B. Khouider, A.J. Majda, A non-oscillatory balanced scheme for an idealized tropical climate model—part II: nonlinear coupling and moisture effects, Theor. Comput. Fluid Dyn. 19 (2005) 355–375.
[16] O.M. Pauluis, D.M.W. Frierson, A.J. Majda, Precipitation fronts and the reflection and transmission of tropical disturbances, Quart. J. R. Meteor. Soc. 134 (2008) 913–930.